

Rab3D and Actin Reveal Distinct Lamellar Body Subpopulations in Alveolar Epithelial Type II Cells

Laura van Weeren, Anko M. de Graaff, James D. Jamieson, Joseph J. Batenburg, and Jack A. Valentijn

Department of Biochemistry and Cell Biology, Faculty of Veterinary Medicine, University of Utrecht, The Netherlands; and Department of Cell Biology, Yale University School of Medicine, New Haven, Connecticut

Rab3D is a small GTP-binding protein associated with secretory vesicles in various exocrine and endocrine cells, where it has been implicated in regulated exocytosis. Data obtained previously in pancreas have suggested that rab3D is involved in the coating of secretory granules with filamentous actin. In the present study we employed Western blot analysis, immunofluorescence, and immunoelectron microscopy to examine the distribution of rab3D in rat lung. Rab3D immunoreactivity was detected in bronchiolar Clara cells and alveolar epithelial type II (AET-II) cells. In both cell types, rab3D displayed preferential localization to secretory vesicles that were identified using specific antibodies against Clara Cell Secretory Protein and p180 lamellar body protein, respectively. Interestingly, rab3D was associated with only 24% of the lamellar bodies in AET-II cells. Rab3D-positive lamellar bodies were typically in close proximity of the apical plasma membrane, where exocytosis occurs. Another subpopulation of lamellar bodies, constituting only 2%, was not only rab3D-positive but could also be labeled with the filamentous-actin probe phalloidin. A third subpopulation, constituting 9%, displayed actin coating without rab3D staining. We propose that these three lamellar body subpopulations represent consecutive intermediates along the regulated exocytotic pathway, implying that rab3D release and actin coating are intimately linked processes.

The respiratory efficiency and homeostasis of the lungs depends on the exocrine function of several secretory cell types. Among these, the alveolar epithelial type II (AET-II) cells release surfactant, a complex mixture of lipids and proteins, into the alveolar space. The presence of a surfactant layer at the air-liquid interface in the alveoli lowers the alveolar surface tension such that the alveoli remain inflated (1). The maintenance of alveolar integrity is a highly regulated process whereby surfactant release is balanced by surfactant reuptake (2, 3). Newly synthesized and recycled surfactant is stored and released by lamellar bodies, which are the specialized secretory vesicles of AET-II cells. The bronchiolar epithelial Clara cells release a number of bio-

active peptides and proteins, including Clara cell secretory protein (CCSP). Although the precise function of Clara cells remains to be established, there is convincing data suggesting that they play an immunomodulatory and anti-inflammatory role (4).

Over the past decade, substantial progress has been made in the unraveling of the molecular mechanisms that underlie membrane fusion processes along the secretory pathway, including exocytosis. Unquestionably, Rothman and coworkers (5) made the most significant contribution to this field by postulating the now widely accepted SNARE (soluble N-ethyl-maleimide sensitive factor [NSF] attachment protein receptor) principle. According to the SNARE hypothesis, each transport vesicle on the secretory pathway carries a specific set of proteins (v-SNAREs) that pair with their cognate receptor on the target membrane (t-SNAREs), thus providing the basis for specificity of membrane interaction. Studies on various secretory cells have revealed that the SNARE machinery is universal and remarkably well conserved in evolution.

In addition to SNARE proteins, many putative regulators of SNARE complexes have been identified in recent years. One of these candidate regulatory proteins is rab3D, a low molecular-weight GTP-binding protein belonging to a subclass of ras-like proteins termed rab proteins (6). Over 60 mammalian rab proteins have been identified so far, and each of them displays organelle-specific localizations and functions (7). As a group, rab proteins and their effectors appear to regulate all forms of intracellular membrane traffic, including vesicular transport along the endocytotic and exocytotic pathways. Newly synthesized rab proteins are modified by the posttranslational addition of a geranylgeranyl group on each of two carboxyterminal cysteines (8). These isoprenoid moieties serve as a lipid anchor allowing for the association of rab proteins with membranes. Several rab proteins, including rab3D, can also undergo reversible carboxymethylation, the function of which remains to be established (9, 10). Rab3D was first characterized in adipocytes, where it has been implicated in Glut4 translocation (11). Subsequently, it was shown that rab3D is abundantly present on the membranes of secretory granules in various exocrine tissues including pancreas and parotid (12, 13).

To this date, little is known about the molecular machinery governing exocytosis in AET-II cells and Clara cells. The present study reports the localization of rab3D to these cells. Our data indicate that rab3D is present on the secretory vesicles of both Clara cells and AET-II cells. In the latter, rab3D was found to associate with only a minor subpopulation of lamellar bodies, suggesting that rab3D plays a role in surfactant secretion, and that this role is transitory in character.

(Received in original form July 16, 2003 and in revised form August 15, 2003)

Address correspondence to: Jack A. Valentijn, Ph.D., Department of Biochemistry and Cell Biology, Faculty of Veterinary Medicine, University of Utrecht, Yalelaan 2, 3584 CM Utrecht, The Netherlands. E-mail: j.a.valentijn@vet.uu.nl

Abbreviations: alveolar epithelial type II cells, AET-II cells; Clara cell secretory protein, CCSP; cysteine string protein, CSP; filamentous actin, F-actin; normal goat serum, NGS; phosphate-buffered saline, PBS; post-nuclear supernatant, PNS; sodium dodecyl sulfate-polyacrylamide gel electrophoresis, SDS-PAGE; soluble N-ethyl-maleimide sensitive factor attachment protein receptor, SNARE; urine protein-1, UP-1.

Am. J. Respir. Cell Mol. Biol. Vol. 30, pp. 288-295, 2004
Originally Published in Press as DOI: 10.1165/rcmb.2003-0264OC on August 21, 2003
Internet address: www.atsjournals.org

Materials and Methods

Animals

Adult male Wistar rats (Harlan, Horst, The Netherlands), weighing 100–150 g, were used as tissue donors. Upon delivery, the rats were housed for at least 1 wk in the Central Animal Laboratory of Utrecht University. Animals were killed via stunning followed by cervical dislocation. Their chest cavities were quickly opened and lung tissue was cleared of blood by perfusion with 0.3 M sucrose. Thereafter, the lung tissue was removed and processed for biochemical or immunocytochemical procedures, as described below.

Antibodies, Fluorescent Probes, and Protein A–Gold Conjugates

Two well-characterized rabbit polyclonal antisera were used to detect rab3D. One was raised against bacterially expressed rab3D (10), and the other against the unique carboxy-terminal peptide sequence of rab3D, SSSPGSNGKGPALGDTPPPQSS (14). Monoclonal antibody clone 3C9 against p180 lamellar body protein was purchased from BABCO (Richmond, CA). Clara cell secretory protein was detected with a rabbit polyclonal antiserum against the highly homologous human urine protein 1 (UPI); the antiserum was procured from DAKO (Glostrup, Denmark). The UPI antiserum was conjugated directly to Alexa-488 fluorochromes using an Alexa Fluor Protein Labeling Kit (Molecular Probes, Leiden, The Netherlands) and following the instructions provided with the kit. Rabbit polyclonal antibodies against cysteine string protein (CSP) were a kind gift of Dr. Cameron B. Gundersen, UCLA School of Medicine, Los Angeles, CA. They were raised against a recombinant construct of rat CSP from which the cysteine-string domain was deleted (15). Secondary goat anti-mouse and goat anti-rabbit antibodies, conjugated with Alexa 350, Alexa 488, or Alexa 568, were obtained from Molecular Probes (Leiden, The Netherlands). Alexa-568 labeled phalloidin was also from Molecular Probes. Protein A conjugated with 5-nm colloidal gold was purchased from the Cell Biology Department of the Utrecht Medical Center in The Netherlands.

Biochemical Procedures

Homogenates of lung tissue were prepared at 0°C in 0.3 M sucrose, 0.5 mM MgCl₂, 25 mM Hepes, pH 6.8, supplemented with Complete protease inhibitor cocktail (Roche Diagnostics, Mannheim, Germany), using a motor-driven Teflon-glass homogenizer. Aliquots of the homogenates were stored at –20°C until further use. Pancreas homogenates used as a positive control were prepared following the same procedure. AET-II cells were isolated from rat lungs according to the method of Dobbs and coworkers (16).

Subcellular fractions were prepared from a postnuclear supernatant (PNS) obtained by centrifugation of fresh homogenate for 15 min at 300 × *g* and 4°C to pellet nuclei and debris. The PNS was spun for 1 h at 200,000 × *g* and 4°C to generate a supernatant fraction, containing the cytosol, and a particulate fraction, containing the membranes. Lamellar bodies were isolated by isopycnic centrifugation of lung homogenates in a linear sucrose gradient using the procedure described by Duck-Chong (17).

Phase separation of hydrophobic and hydrophilic proteins with Triton X-114 was performed on PNS samples according to Bordier (18).

Homogenates, subcellular fractions, and Triton X-114-extracted samples were resolved by sodium dodecyl sulfate–polyacrylamide gel electrophoresis (SDS-PAGE). For this purpose, samples were normalized for protein content, diluted in Laemmli reducing buffer, and boiled for 4 min. The samples were subsequently electro-

phoresed on 12% polyacrylamide gels, electrotransferred to polyvinylidene fluoride (PVDF) membranes (Bio-Rad, Veenendaal, The Netherlands) and immunoblotted with rab3D antisera using a chemiluminescence detection system (Roche Diagnostics).

Immunofluorescence Procedures

Small pieces of lung tissue, ~ 1 mm³ in size, were immersion-fixed overnight at 4°C with 4% paraformaldehyde in 0.3 M sucrose and 5 mM phosphate buffer, pH 7.4. They were rinsed in 50 mM Tris buffer, pH 7.4, mounted in tissue freezing medium and frozen to –20°C. Frozen sections, 5–8 μm thick, were cut on a Leica CM3050 Cryostat (Leica Microsystems, Nussloch, Germany). The sections were collected on SuperFrost microscope slides (Menzel-Gläser, Braunschweig, Germany) and stored at –20°C until further use. For immunohistochemistry, thawed sections were rinsed 15 min with 50 mM Tris buffer, pH 7.4, 3 × 5 min with phosphate-buffered saline (PBS; 0.15 M NaCl, 20 mM phosphate buffer, pH 7.4) containing 0.1% Triton X-100, and incubated 30 min with 5% normal goat serum (NGS) in PBS to reduce background staining. Primary antibodies were diluted in PBS/Triton X-100 containing 5% NGS and incubated on the tissue sections for 3–4 h. Secondary antibodies were also diluted in PBS/Triton X-100 containing 5% NGS but were incubated on the sections for 1 h. In between the primary and secondary antibody incubations, sections were rinsed 3 × with PBS/Triton X-100. In double-label experiments using a mouse and a rabbit primary antibody, the antibodies were incubated as a cocktail. The results obtained via this protocol were not different from experiments where the antibodies were incubated sequentially. Phalloidin staining was performed at the end of primary and secondary antibody incubations. Phalloidin was diluted 1:25 in PBS/Triton X-100 and incubated on the sections for 30 min. At the end of the labeling reactions, sections were thoroughly rinsed with PBS/Triton X-100 and embedded in Fluorsave mounting medium (Calbiochem, San Diego, CA).

Fluorescent signals were visualized using either a Leica TCS SP confocal laser-scanning microscope or a Bio-Rad Radiance 2100MP confocal and multi-photon system (Bio-Rad, Hertfordshire, UK) equipped with a Nikon TE300 inverted microscope (Uvikon, Bunnik, Netherlands). On the latter imaging system, excitation of the Alexa 350 probes was achieved by multi-photon excitation at 750 nm using a mode-locked Titanium:Sapphire laser (Tsunami; Spectra-Physics, Mountain View, CA) pumped by a 10 W solid state laser (Millennia Xs; Spectra-Physics), whereas the Alexa 488 and 568 probes were excited by confocal lasers.

Immunolectron Microscopy

Ultrastructural localization of rab3D was performed using pre-embedding immunocytochemistry. Small pieces of lung tissue (volume ~ 1 mm³) were immersed overnight at 4°C in fixative (4% paraformaldehyde in 0.3 M sucrose and 5 mM phosphate buffer, pH 7.4). Subsequently, the tissue fragments were washed 2 × 5 min and cryoprotected for 6 h in 30% sucrose, after which they were permeabilized by three successive freeze–thaw cycles (freezing in liquid nitrogen, thawing at room temperature). The fragments were then washed for 5 min in PBS and incubated overnight at 4°C in rab3D antiserum at a dilution of 1:50 in PBS containing 0.1% acetylated BSA (Aurion, Wageningen, the Netherlands). Next they were washed 3 × 10 min in PBS and incubated for 4 h with 5-nm colloidal gold-conjugated protein A at a dilution of 1:75 in PBS. After washing 5 × 10 min in PBS followed by 10 min in 0.1 M cacodylate buffer, pH 7.4, the tissue fragments were post-fixed overnight with 2% glutaraldehyde in 0.1 M cacodylate buffer, washed in 0.1 M cacodylate buffer, and post-fixed again for 2 h with 2% osmium tetroxide

in 0.1 M cacodylate buffer. They were then washed in distilled water, block stained for 1 h with 2% uranyl acetate, dehydrated in a graded acetone series, and infiltrated with Durcupan resin. After hardening of the resin at 60°C, 70–100 nm ultrathin sections were cut on a Reichert Ultracut S ultramicrotome and collected on 200-mesh copper grids. The sections were viewed and photographed with a Philips CM10 transmission electron microscope.

Image Processing

Raw images acquired by the photomultipliers of the confocal and multiphoton systems were enhanced in Adobe Photoshop. The enhancements consisted of minor adjustments to the dynamic range (levels settings) and of pixel shifting to correct for subtle differences between the alignment of the multiphoton and the confocal lasers.

Electron micrograph negatives were scanned at high resolution and bit depth on a Heidelberg Linoscan 1450 flatbed scanner. The thus obtained 12-bit images were adjusted for dynamic range and subsequently sampled down to 8-bit.

Results

Detection of rab3D protein in rat lung was performed using a well-characterized antiserum raised against recombinant rab3D. As reported previously, this serum does not cross-react with the rab3 isoforms, rab3A, rab3B, and rab3C (14). On Western blots of lung homogenates submitted to SDS-PAGE, the rab3D antiserum recognized two protein bands (Figure 1A). The lower band ran at ~27 kD, which corresponds to the published molecular weight of rab3D (11), and comigrated with the rab3D band in pancreas homogenates run as a positive control. The 27-kD band was also detected by an antiserum raised against the unique C-terminal peptide sequence of rab3D (Figure 1B). It thus appeared that rat lung tissue expresses a rab3D-like protein. Whether the higher band of ~40 kD, which was detected by both antisera, is immunologically related to rab3D or represents a distinct protein recognized by a contaminating antibody species, remains to be determined.

Because rab3D is a marker of secretory vesicles, particularly in exocrine cells, we explored the possibility that the rab3D detected in lung homogenates was the product of the surfactant-secreting AET-II cells. For this purpose, AET-II cells were isolated from lung tissue, resolved by SDS-PAGE, and analyzed on Western blot for the presence of rab3D-immunoreactivity. In addition, the secretory compartments of AET-II cells, lamellar bodies, were purified from lung homogenates by isopycnic centrifugation in a linear sucrose gradient. The lamellar body fractions were also submitted to SDS-PAGE and immunoblot analysis. As shown in Figure 1A, rab3D was detected in both AET-II cells and lamellar body fractions. However, AET-II cells gave a much weaker signal for rab3D than lung homogenates when samples with equal protein content were compared. Similarly, the lamellar body fractions needed to be concentrated by a factor of 10–20 to yield a signal for rab3D that was comparable in intensity to that produced by the lung homogenates from which the lamellar bodies were purified. These data suggested that although AET-II cells expressed rab3D, there was another source of rab3D in lung tissue.

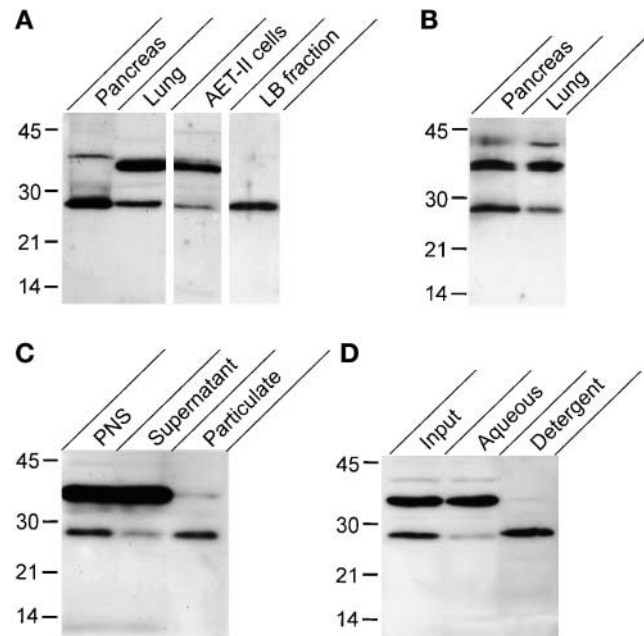


Figure 1. Immunoblot detection of rab3D in lung. (A) An antiserum, raised against recombinant rab3D, detected a ~27-kD protein band in homogenates of lung, purified AET-II cells, and purified lamellar bodies (LB fraction). The electrophoretic mobility of this band was identical to that of rab3D in pancreas homogenate used as a positive control. Sample loads in each lane were equivalent to 40 μ g total protein, except for the lamellar body fraction, which was equivalent to 800 μ g total protein in the homogenate from which the fraction was derived. Note that neither the AET-II cell nor the LB fractions were enriched in rab3D immunoreactivity. The rab3D antiserum also recognized a protein band of ~40 kD, the nature of which is unknown. Note that this higher band was absent in the LB fraction. (B) Another antiserum, raised against the unique C-terminal peptide sequence of rab3D, yielded comparable results. (C) Following high-speed centrifugation of post-nuclear supernatant (PNS), rab3D was recovered mainly in the particulate fraction (containing the membranes), whereas the higher band of ~40 kD partitioned into the supernatant fraction (containing the cytosol). Sample loads in each lane were equivalent to 40 μ g total protein in the PNS. Antiserum used was identical to that in A. (D) Following Triton X-114 phase separation of PNS, rab3D partitioned mainly into the detergent phase, whereas the higher band partitioned into the aqueous phase. Sample loads in each lane were equivalent to 40 μ g total protein in the post-nuclear supernatant used as input sample. Antiserum used was identical to that in A.

To examine the distribution of rab3D over membranes and cytosol, we prepared subcellular fractions by centrifugation (200,000 \times g for 1 h) of postnuclear supernatants generated from lung homogenates. The majority of rab3D immunoreactivity was associated with the particulate fraction containing the membranes. In contrast, the higher band detected by the rab3D antiserum was recovered in the supernatant fraction (Figure 1C). Likewise, the majority of rab3D partitioned into the detergent phase following Triton X-114 phase separation, whereas the higher band partitioned into the aqueous phase (Figure 1D). The predominant membrane association of rab3D and partitioning into the detergent phase is in agreement with previous findings in pancreas (13, 19).

More detailed information on the localization of rab3D in rat lung was gathered by employing immunofluorescence microscopic techniques. Because the higher band detected by the rab3D antiserum behaved as a cytosolic rather than a membrane-bound protein, there was no incentive against using this antiserum for the specific localization of membrane-associated rab3D. In a first series of experiments, 5–8 μm thick cryostat sections cut from 4% paraformaldehyde-fixed lung tissue were immunodecorated with the rab3D antiserum and fluorochrome-labeled secondary antibodies. Confocal laser-scanning microscopy revealed that rab3D immunoreactivity was present in at least two distinct cell types. One of these cell types, found predominantly in respiratory bronchioles, appeared nonciliated under phase-contrast illumination and was reminiscent of the secretory Clara cells. The rab3D antiserum produced a vesicular staining pattern in the apical region of these cells (Figure 2). The staining pattern overlapped with that of an antiserum against CCSP, a marker of the secretory granules of Clara cells (Figure 2). This observation indicated that rab3D localizes to the secretory granule membranes of Clara cells.

The second cell type that displayed rab3D immunoreactivity was found in lung alveoli. The rab3D staining pattern in these cells was mostly punctate. Rab3D-immunoreactive punctae were scattered throughout the cytoplasm and also appeared to be associated with the apical plasma membrane facing the alveolar space (Figure 3). Regularly, the rab3D antiserum labeled the outlines of vesicular structures with diameters ranging from 0.5–1 μm . These vesicular structures also reacted with monoclonal antibody 3C9, which recognizes p180, a marker of the limiting membrane of lamellar bodies (Figure 3). It thus became evident that AET-II cells represented the second cell type in lung displaying rab3D

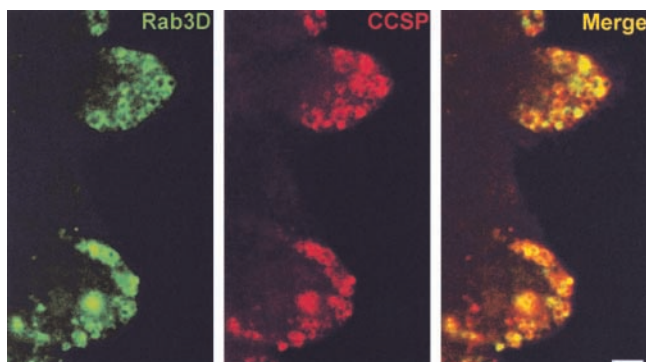


Figure 2. Rab3D localizes to secretory granules in Clara cells. Cryostat sections of fixed lung tissue were double-labeled with antisera against rab3D and CCSP. A typical example is shown of the staining pattern produced by the rab3D and CCSP antisera in optical sections through nonciliated cells lining respiratory bronchioles. In the two cells depicted, rab3D immunoreactivity (shown in green) outlines vesicular structures in the apical area. These structures are also immunoreactive for CCSP (shown in red). Overlap between the rab3D and CCSP staining patterns is demonstrated by the yellow color in the Merge pane. Although one would expect the CCSP antibodies to label the cores of the vesicles, they often appear to label only the outlines. This is probably due to limited antibody penetration into the cores. Scale bar represents 2 μm .

immunoreactivity. Interestingly, the lamellar bodies that were immunoreactive for rab3D constituted a relatively small subpopulation. In fact, out of a total of 1,267 3C9-labeled lamellar bodies counted in optical sections through 253 randomly chosen AET-II cells, only 299 (24%) were positive for rab3D.

The finding that only a minor subpopulation of lamellar bodies exhibited immunoreactivity for rab3D was rather unexpected because it was different from other secretory cells expressing rab3D, such as pancreatic acinar cells, where zymogen granules carrying rab3D are preponderant. We were therefore compelled to consider the possibility that rab3D, which presumably is tethered to the outer membrane leaflet via lipid moieties, might have been extracted from lamellar bodies during the immunohistochemical procedures. As a control, we conducted a set of identical experiments using an antiserum raised against CSP. This protein is comparable in size (34 kD) to rab3D, also possesses lipid modifications required for attachment to the outer membrane leaflet, and associates with secretory vesicles of various cell types. Figure 3D illustrates that the CSP antiserum immunodecorated the entire lamellar body population as revealed by 3C9 labeling. It thus seemed unlikely that the distinctive rab3D localization in AET-II cells was attributable to an artifact.

The intricacy of the rab3D staining pattern observed in AET-II cells at the light microscopic level urged the employment of immunoelectron-microscopic techniques to obtain ultrastructural information on the localization of rab3D. Using the same antiserum as in the above-described experiments, we detected protein-A–gold labeling on the delimiting membrane of a minor subpopulation of lamellar bodies in AET-II cells (Figure 4). These rab3D-positive lamellar bodies were most often encountered in the proximity of the apical plasma membrane. Multivesicular bodies, which are closely related to lamellar bodies, were devoid of immunogold labeling (data not shown). In contrast, rab3D labeling was located on tubules and vesicles in the trans-Golgi network area (Figure 4B). Furthermore, rab3D-immunoreactivity was present on small (50–100 nm) vesicles scattered throughout the cytoplasm of AET-II cells (Figure 4C). Similar rab3D-positive vesicles were observed in close proximity of the apical plasma membrane (Figure 4C). On occasion, rab3D-positive small vesicles were found adjoining lamellar bodies (Figure 4C). It thus appeared that the punctate cytoplasmic staining for rab3D observed by immunofluorescence was equivalent to the immunogold-labeled vesicles and tubules detected at the electron microscope level.

It has been shown in pancreatic acinar cells that a number of zymogen granules are devoid of rab3D under conditions where secretory activity is stimulated. Interestingly, these rab3D-negative zymogen granules are coated with filamentous actin (F-actin), whereas the rab3D-positive granules lack F-actin coating (20). This and other findings led to the hypothesis that zymogen granules engaging in exocytosis first shed rab3D and subsequently become coated with F-actin (20). We were thus prompted by the question whether an analogous phenomenon existed in AET-II cells. Therefore we set about to study the distribution of F-actin in AET-II cells, with particular emphasis on the possible

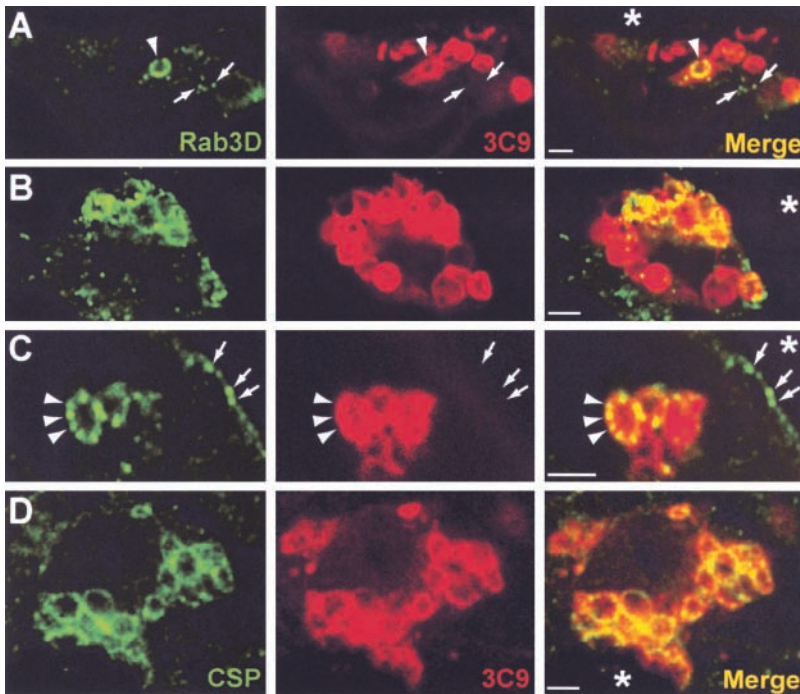


Figure 3. Rab3D localization in AET-II cells by immunofluorescence. Cryostat sections of fixed lung tissue were double-labeled with rab3D antiserum and monoclonal antibody 3C9, which recognizes p180, a marker of the limiting membrane of lamellar bodies. Rab3D-immunoreactivity is shown in green, whereas 3C9-labeling is shown in red. Overlap between the rab3D and 3C9 staining-patterns is demonstrated by the yellow color in the Merge panes. Asterisks indicate the alveolar space. Scale bars represent 2 μ m. (A) Typical example of an AET-II cell displaying numerous 3C9-labeled lamellar bodies, one of which is also positive for rab3D (arrowhead). Note that in addition to labeling a lamellar body, the rab3D antiserum also produces a punctate staining pattern throughout the cytoplasm. Arrows highlight two immunoreactive punctae. (B) Example of a less frequently occurring AET-II cell in which several 3C9-positive lamellar bodies display rab3D-immunoreactivity. (C) Close-up of the apical region of an AET-II cell with rab3D-immunoreactive lamellar bodies, illustrating the punctate nature of the rab3D-staining (arrowheads). The cell boundary, i.e., the plasma membrane, is also lined by rab3D-positive punctae (arrows). (D) Localization of CSP as a control for the intermittent lamellar body labeling for rab3D. Sections were double-labeled with CSP antiserum (shown in green) and monoclonal antibody 3C9 (shown in red). Overlap between the CSP and 3C9 staining-patterns is demonstrated by the yellow color in the Merge panes. Note that in contrast to rab3D, the CSP antiserum labels all 3C9-positive lamellar bodies.

association of F-actin with lamellar bodies. As illustrated in Figure 5, the F-actin probe phalloidin labeled a subpopulation of lamellar bodies. These actin-coated lamellar bodies were almost exclusively found in close proximity of the apical plasma membrane. Out of 1,340 3C9-labeled lamellar bodies counted in optical sections through 260 randomly chosen AET-II cells, 114 (9%) displayed coating with F-actin. The question now arose as to whether actin-coated and rab3D-positive lamellar bodies formed distinct or overlapping subpopulations. To answer this question, we performed triple labeling with 3C9 antibodies, rab3D antiserum, and phalloidin, on cryostat sections of fixed lung tissue. Typical examples of the staining patterns we observed are shown in Figure 6. Out of 1,185 3C9-labeled lamellar bodies counted in optical sections through 227 cells selected for the presence of rab3D-positive lamellar bodies, 27 (2%) displayed labeling for both rab3D and phalloidin, whereas 356 (30%) labeled with rab3D antiserum alone and 115 (10%) with phalloidin alone. These values indicated that rab3D and F-actin rarely coexisted on the same lamellar body, and that the majority of rab3D-positive lamellar bodies formed a subpopulation that was distinct from actin-coated lamellar bodies. In addition, they indicated that the largest population of lamellar bodies, \sim 60%, was devoid of rab3D-immunoreactivity as well as phalloidin-binding.

Discussion

Lung tissue has been identified as a major source of mRNA encoding the small GTP-binding protein rab3D (21). In

contrast, a recent study employing quantitative immunoblotting to map the tissue distribution of rab3 isoforms failed to detect rab3D protein in Triton X-114 extracts of lung tissue (22). Here, on the other hand, we demonstrate that rab3D is expressed at the protein level in two of the principal secretory cell types present in lung, Clara cells, and AET-II cells. The discrepancy of our data with the study by Schluter and colleagues (22) probably results from differences in sample preparation or sensitivity of the detection systems used. Rab3D displayed localization to secretory granules in Clara cells as well as AET-II cells, which is in concordance with the distribution of rab3D in other secretory cells, including acinar cells of pancreas (13), parotid (12), and lacrimal gland (12), mast cells (23), and gastric chief cells (24). Although the identification of rab3D as a specific marker of Clara cell secretory granules merits further analysis, the present study focused primarily on the characterization of rab3D in AET-II cells because of the peculiar and hence interesting distribution of rab3D in these cells, as will be discussed below.

The surfactant-containing lamellar bodies of AET-II cells form a unique class of storage and secretory vesicles, displaying characteristics of lysosomes and late endosomes (25). Their biogenesis appears to involve fusion of multivesicular bodies containing newly synthesized surfactant components derived from the ER-Golgi route and recycled surfactant components delivered via the endocytotic pathway (26). Little is known about the molecular machinery governing exocytosis of lamellar bodies (27). Zimmerman

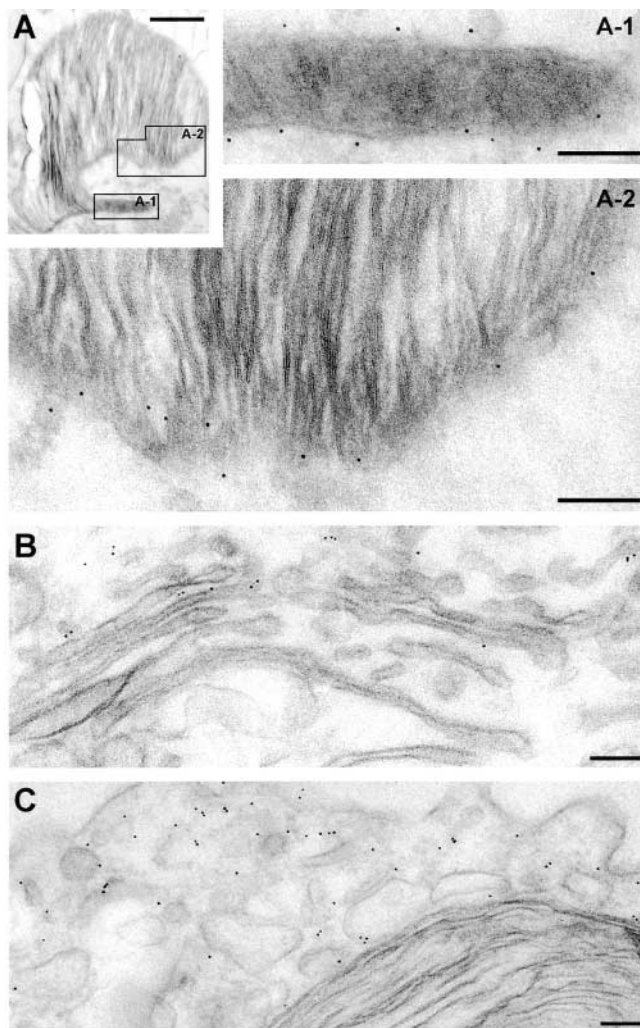


Figure 4. Rab3D localization in AET-II cells by pre-embedding immunogold detection. (A) Typical example of a lamellar body displaying immunogold labeling with rab3D antiserum and 5-nm protein-A-gold. Because of the relatively large size of lamellar bodies compared with the gold particles, the labeling can only be appreciated in close-ups. The close-ups A-1 and A-2 correspond to the areas in the boxes A-1 and A-2 drawn on the overview. In total 48 gold grains surrounded the lamellar body shown here. (B) Typical example of immunogold labeling for rab3D of tubules and vesicles in the trans-Golgi network area of an AET-II cell. (C) Typical example of rab3D labeling in the subapical region of an AET-II cell. Various small vesicles are decorated by rab3D-immunogold. Note that some of these rab3D-positive vesicles are adjoining the lamellar body that is partially shown in the *bottom right corner*. Scale bars represent 0.5 μm in A, and 0.1 μm in A-1, A-2, B, and C.

and coworkers (28) reported on the presence of the SNARE proteins VAMP-2, SNAP-25, and syntaxin in AET-II cells, while Abonyo and colleagues (29) recently implicated the SNARE regulators, α -SNAP and NSF, in secretion of pulmonary surfactant. Herein we expand the list of SNARE-related proteins present in AET-II cells with rab3D and CSP, two putative regulators of SNARE-mediated exo-

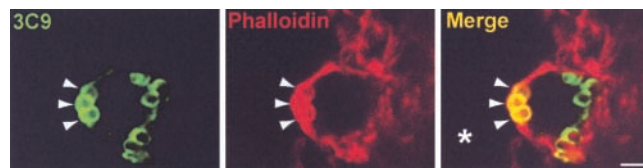


Figure 5. A subpopulation of lamellar bodies is surrounded by F-actin. Cryostat sections of fixed lung tissue were double-labeled with the fluorescent F-actin probe, Alexa-568 phalloidin, and monoclonal antibody 3C9, which recognizes p180, a marker of the limiting membrane of lamellar bodies. 3C9-immunoreactivity is shown in *green*, whereas phalloidin-labeling is shown in *red*. Overlap between the 3C9 and phalloidin staining-patterns is demonstrated by the *yellow color* in the Merge pane. The optical section through an AET-II cell depicted in this typical example displays numerous 3C9-positive lamellar bodies, three of which are also labeled with phalloidin (*arrowheads*). Note that these phalloidin-labeled lamellar bodies are all in close proximity of the actin terminal web lining the apical plasma membrane. The *asterisk* indicates the alveolar space. The *scale bar* represents 2 μm .

cytosis. Rab3D and CSP were both associated with lamellar bodies, a finding that is of particular interest in the light of a recent study in which a functional link has been established between CSP and rab proteins (30). Namely, it was demonstrated that synaptic membranes contain a chaperone complex composed of CSP, Hsc70, Hsp90, and rab-specific α -GDP-dissociation inhibitor (α -GDI), and that this complex regulates the recycling of rab3A and Ca^{2+} -dependent neurotransmitter release. It is thus conceivable that the CSP present on lamellar bodies regulates the association and dissociation of rab3D. We are currently addressing this hypothesis. Preliminary data indicate that specific inhibitors of Hsp90 cause a dramatic increase in rab3D labeling of the apical plasma membrane area.

Strikingly, rab3D was detected on only about a quarter of the lamellar bodies. This finding indicates the existence of biochemically distinct subpopulations of lamellar bodies. To the best of our knowledge, this is the first evidence for such heterogeneity among lamellar bodies in AET-II cells. The functional significance of the existence of rab3D-positive and rab3D-negative lamellar bodies remains to be established. However, given that rab3D-positive lamellar bodies were usually in close proximity to the apical plasma membrane where exocytosis takes place, it is likely that they constitute a pool of mature secretory granules ready for exocytosis. In agreement with this hypothesis, we found that rab3D was absent on multivesicular bodies, whose fusion with lamellar bodies is thought to represent the underlying mechanism of lamellar body maturation. Taken together, these data indicate that a control system exists in AET-II cells to single out mature lamellar bodies and flag them with rab3D. How these lamellar bodies acquire rab3D remains to be determined, but it is conceivable that rab3D is recruited either from the cytosol or from the small rab3D-positive vesicles we occasionally observed adjoining lamellar bodies. There is an interesting parallel that can be drawn between the maturation of lamellar bodies and that of phagosomes in professional phagocytes. In the latter, nascent and early

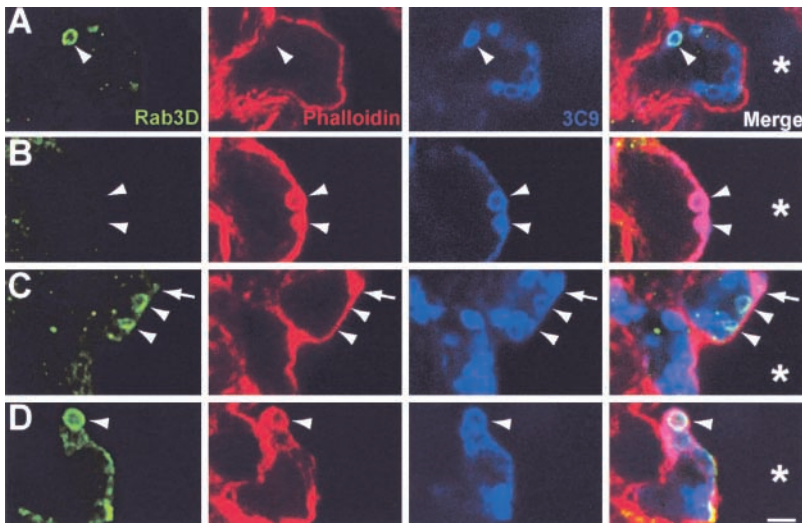


Figure 6. Four distinct subpopulations of lamellar bodies revealed on the basis of differential labeling with rab3D antibodies and phalloidin. Cryostat sections of fixed lung tissue were triple-labeled with the fluorescent F-actin probe, Alexa-568 phalloidin, polyclonal rab3D antiserum, and monoclonal antibody 3C9. Rab3D-immunoreactivity is shown in green, phalloidin-labeling is shown in red, and 3C9-immunoreactivity in blue. The overlays of the green, red, and blue channels are shown in the Merge panes. (A) Optical section through an AET-II cell showing a rab3D-positive, phalloidin-negative lamellar body (arrowhead). Note that the 3C9 staining reveals several lamellar bodies not labeled for rab3D or phalloidin. (B) An optical section through another AET-II cell reveals two phalloidin-labeled lamellar bodies (arrowheads); both are rab3D-negative. Note that the phalloidin-labeled lamellar bodies are in close proximity of the actin terminal web lining the apical plasma membrane. The cell also contained phalloidin-

negative lamellar bodies, but they were present in separate optical sections. (C) This example shows, in one optical section, rab3D-positive, phalloidin-negative lamellar bodies (arrowheads), and a phalloidin-positive, rab3D-negative lamellar body (arrow). Other lamellar bodies are negative for both rab3D and phalloidin. Note that the rab3D-positive as well as the phalloidin-positive lamellar bodies are in close proximity of the apical plasma membrane. (D) Example of an optical section through an AET-II cell containing a lamellar body (arrowhead) that is positive for both rab3D and phalloidin. Lamellar bodies of this type belonged to the most infrequently encountered. Asterisks indicate the alveolar space. Scale bars represent 2 μ m.

phagosomes lack rab7 but acquire this small GTPase at a later stage of maturation, where it may mediate the transition between early and late phagosomes or phagolysosomes (31). Incidentally, rab7, a marker of late endosomes, has also been detected on lamellar bodies (25), but it is not yet clear whether rab7 localizes to the whole population or just a subpopulation of lamellar bodies.

The additional localization of rab3D on small vesicles in the trans-Golgi network area of AET-II cells is difficult to reconcile with the above data. A similar localization of rab3D to elements of the trans-Golgi network has been described in pancreatic acinar cells (13), suggesting that it is a general phenomenon in rab3D-expressing cells. These data would rather suggest a role for rab3D in an early step of secretory granule maturation. Moreover, it has recently been shown that secretagogue-induced zymogen granule discharge by pancreatic acinar cells remains normal in rab3D-deficient mice, whereas the size of zymogen granules nearly doubles (32), thus implicating rab3D again in the biogenesis of secretory vesicles. Clearly, further data will be needed to arrive at a unifying hypothesis explaining the function of rab3D in the context of its diverse localizations. Nevertheless, we are tempted to speculate that the TGN-associated rab3D originates from exocytosed lamellar bodies and functions as a signal for the TGN to produce cargo vesicles containing components that are required by lamellar bodies during maturation. The advantage of such a signaling pathway would be that the amount of cargo vesicles produced is proportional to the rate of exocytosis.

Another issue that complicates the clarification of rab3D function is the apparent interaction of rab3D with the actin cytoskeleton. Evidence is accumulating that rab proteins establish a link between transport vesicles and the cytoskeleton. In particular, several rab proteins have been con-

nected to microtubule- and actin-based motor proteins (33). The most elegant demonstration of such interaction to date is that of rab27a, which tethers melanosomes to both actin filaments and microtubules, using as intermediate melanophilin, which binds to the actin-motor myosin Va, which in turn forms a complex with the microtubule-motor kinesin (34). Although the current evidence for an interaction between rab3D and the actin cytoskeleton is circumstantial in nature, it merits further investigation. It was found in pancreatic acinar cells that upon secretagogue stimulation, zymogen granules in proximity of the apical plasma membrane shed rab3D and subsequently become coated with filamentous actin, while modulators of the actomyosin system can prevent the loss of rab3D from actin-coated granules (20). Tsilibary and Williams (35) have previously shown by transmission electron microscopy that lamellar bodies, including lamellar bodies undergoing exocytosis, are surrounded by actin-like material. We herein confirm the existence of actin-coated lamellar bodies by using fluorescent phalloidin to label F-actin. Our data further indicate that only a subpopulation of lamellar bodies, constituting $\sim 10\%$ of the 3C9-positive lamellar bodies, displayed actin coating. Consistent with previous findings in exocrine pancreas, the majority of the actin-coated lamellar bodies lacked rab3D-labeling. Still, a non-negligible 2% of lamellar bodies carried rab3D as well as F-actin, suggesting that rab3D-labeled lamellar bodies progress into actin-coated lamellar bodies via a relatively short-lived intermediate state where rab3D and F-actin co-localize. As will be reported elsewhere, recent data from our laboratory show that the myosin ATPase inhibitor, 2,3-butanedione monoxime (BDM), causes a dramatic increase in the number of rab3D-positive lamellar bodies. In addition, we found that the combined administration of BDM and the actin-disrupting agent, latrunculin

A, leads paradoxically to an increase in the number of actin-coated lamellar bodies, many of which are rab3D-positive as well. Clearly, the function of rab3D is tightly linked to the actomyosin system, but the precise nature of this interaction remains to be established.

Acknowledgments: The authors are grateful to Mr. Anton Ultee for expert technical assistance. The authors also wish to thank Prof. Lambert M. G. van Golde (University of Utrecht) for critically reading the manuscript, and Dr. Cameron B. Gundersen (UCLA School of Medicine) for helpful discussions and for the generous supply of CSP antibodies. All microscopy was carried out within the Center for Cell Imaging in the Department of Biochemistry and Cell Biology.

References

- Goerke, J., and J. A. Clements. 1986. Alveolar surface tension and lung surfactant. In A. P. Fishman, editor. *Handbook of Physiology, The Respiratory System. Mechanics of Breathing*. Oxford University Press, Bethesda. 247–261.
- Rooney, S. A., S. L. Young, and C. R. Mendelson. 1994. Molecular and cellular processing of lung surfactant. *FASEB J.* 8:957–967.
- Batenburg, J. J., and H. P. Haagsman. 1998. The lipids of pulmonary surfactant: dynamics and interactions with proteins. *Prog. Lipid Res.* 37:235–276.
- Singh, G., and S. L. Katyal. 2000. Clara cell proteins. *Ann. NY Acad. Sci.* 923:43–58.
- Rothman, J. E. 2002. Lasker Basic Medical Research Award. The machinery and principles of vesicle transport in the cell. *Nat. Med.* 8:1059–1062.
- Millar, A. L., N. J. Pavios, J. Xu, and M. H. Zheng. 2002. Rab3D: a regulator of exocytosis in non-neuronal cells. *Histol. Histopathol.* 17:929–936.
- Pfeffer, S. R. 2001. Rab GTPases: specifying and deciphering organelle identity and function. *Trends Cell Biol.* 11:487–491.
- Kinsella, B. T., and W. A. Maltese. 1991. Rab GTP-binding proteins implicated in vesicular transport are isoprenylated in vitro at cysteines within a novel carboxyl-terminal motif. *J. Biol. Chem.* 266:8540–8544.
- Bergo, M. O., G. K. Leung, P. Ambroziak, J. C. Otto, P. J. Casey, A. Q. Gomes, M. C. Seabra, and S. G. Young. 2001. Isoprenylcysteine carboxyl methyltransferase deficiency in mice. *J. Biol. Chem.* 276:5841–5845.
- Valentijn, J. A., and J. D. Jamieson. 1998. Carboxyl methylation of rab3D is developmentally regulated in the rat pancreas: correlation with exocrine function. *Eur. J. Cell Biol.* 76:204–211.
- Baldini, G., T. Hohl, H. Y. Lin, and H. F. Lodish. 1992. Cloning of a Rab3 isotype predominantly expressed in adipocytes. *Proc. Natl. Acad. Sci. USA* 89:5049–5052.
- Ohnishi, H., S. A. Ernst, N. Wys, M. McNiven, and J. A. Williams. 1996. Rab3D localizes to zymogen granules in rat pancreatic acini and other exocrine glands. *Am. J. Physiol.* 271:G531–G538.
- Valentijn, J. A., D. Sengupta, F. D. Gumkowski, L. H. Tang, E. M. Konieczko, and J. D. Jamieson. 1996. Rab3D localizes to secretory granules in rat pancreatic acinar cells. *Eur. J. Cell Biol.* 70:33–41.
- Qiu, X., J. A. Valentijn, and J. D. Jamieson. 2001. Carboxyl-methylation of Rab3D in the rat pancreatic acinar tumor cell line AR42J. *Biochem. Biophys. Res. Commun.* 285:708–714.
- Poage, R. E., S. D. Meriney, C. B. Gundersen, and J. A. Umbach. 1999. Antibodies against cysteine string proteins inhibit evoked neurotransmitter release at *Xenopus* neuromuscular junctions. *J. Neurophysiol.* 82: 50–59.
- Dobbs, L. G., R. Gonzalez, and M. C. Williams. 1986. An improved method for isolating type II cells in high yield and purity. *Am. Rev. Respir. Dis.* 134:141–145.
- Duck-Chong, C. G. 1978. The isolation of lamellar bodies and their membranous content from rat lung, lamb tracheal fluid and human amniotic fluid. *Life Sci.* 22:2025–2030.
- Bordier, C. 1981. Phase separation of integral membrane proteins in Triton X-114 solution. *J. Biol. Chem.* 256:1604–1607.
- Valentijn, J. A., F. D. Gumkowski, and J. D. Jamieson. 1996. The expression pattern of rab3D in the developing rat exocrine pancreas coincides with the acquisition of regulated exocytosis. *Eur. J. Cell Biol.* 71:129–136.
- Valentijn, J. A., K. Valentijn, L. M. Pastore, and J. D. Jamieson. 2000. Actin coating of secretory granules during regulated exocytosis correlates with the release of rab3D. *Proc. Natl. Acad. Sci. USA* 97:1091–1095.
- Adachi, R., R. Nigam, M. J. Tuvim, F. DeMayo, and B. F. Dickey. 2000. Genomic organization, chromosomal localization, and expression of the murine RAB3D gene. *Biochem. Biophys. Res. Commun.* 273:877–883.
- Schluter, O. M., M. Khvotchev, R. Jahn, and T. C. Sudhof. 2002. Localization versus function of Rab3 proteins. Evidence for a common regulatory role in controlling fusion. *J. Biol. Chem.* 277:40919–40929.
- Tuvim, M. J., R. Adachi, J. F. Chocano, R. H. Moore, R. M. Lampert, E. Zera, E. Romero, B. J. Knoll, and B. F. Dickey. 1999. Rab3D, a small GTPase, is localized on mast cell secretory granules and translocates to the plasma membrane upon exocytosis. *Am. J. Respir. Cell Mol. Biol.* 20:79–89.
- Tang, L. H., F. D. Gumkowski, D. Sengupta, I. M. Modlin, and J. D. Jamieson. 1996. rab3D protein is a specific marker for zymogen granules in gastric chief cells of rats and rabbits. *Gastroenterology* 110:809–820.
- Wasano, K., and Y. Hirakawa. 1994. Lamellar bodies of rat alveolar type 2 cells have late endosomal marker proteins on their limiting membranes. *Histochemistry* 102:329–335.
- Williams, M. C. 1984. Uptake of lectins by pulmonary alveolar type II cells: subsequent deposition into lamellar bodies. *Proc. Natl. Acad. Sci. USA* 81:6383–6387.
- Rooney, S. A. 2001. Regulation of surfactant secretion. *Comp. Biochem. Physiol. A Mol. Integr. Physiol.* 129:233–243.
- Zimmerman, U. J., S. K. Malek, L. Liu, and H. L. Li. 1999. Proteolysis of synaptobrevin, syntaxin, and SNAP-25 in alveolar epithelial type II cells. *IUBMB Life* 48:453–458.
- Abonyo, B. O., P. Wang, T. A. Narasaraaju, I. W. Rowan, D. H. McMillan, U. J. Zimmerman, and L. Liu. 2003. Characterization of α -SNAP in alveolar type II cells: implications in lung surfactant secretion. *Am. J. Respir. Cell Mol. Biol.* 29:273–282.
- Sakisaka, T., T. Meerlo, J. Matteson, H. Plutner, and W. E. Balch. 2002. Rab-alphaGDI activity is regulated by a Hsp90 chaperone complex. *EMBO J.* 21:6125–6135.
- Vieira, O. V., R. J. Botelho, and S. Grinstein. 2002. Phagosome maturation: aging gracefully. *Biochem. J.* 366:689–704.
- Riedel, D., W. Antonin, R. Fernandez-Chacon, G. Alvarez de Toledo, T. Jo, M. Geppert, J. A. Valentijn, K. Valentijn, J. D. Jamieson, T. C. Sudhof, and R. Jahn. 2002. Rab3D is not required for exocrine exocytosis but for maintenance of normally sized secretory granules. *Mol. Cell Biol.* 22:6487–6497.
- Goud, B. 2002. How Rab proteins link motors to membranes. *Nat. Cell Biol.* 4:E77–E78.
- Wu, X. S., K. Rao, H. Zhang, F. Wang, J. R. Sellers, L. E. Matesic, N. G. Copeland, N. A. Jenkins, and J. A. Hammer, III. 2002. Identification of an organelle receptor for myosin-Va. *Nat. Cell Biol.* 4:271–278.
- Tsilibary, E. C., and M. C. Williams. 1983. Actin in peripheral rat lung: S1 labeling and structural changes induced by cytochalasin. *J. Histochem. Cytochem.* 31:1289–1297.